Design and Implementation of a Novel 5G Hairpin Bandpass Filter with Defected Ground Structure

Original Scientific Paper

Shereen Abdalkadum Shandal*
Department of Computer Techniques Engineering
Middle Technical University, Baghdad, Iraq
Shereen@mtu.edu.iq

*Corresponding author

Abstract *– In this paper, a three-pole hairpin resonator is designed, simulated, and fabricated on the top layer of the FR4 substrate. Recent trends in miniature size and improved filter performance, particularly in terms of scattering parameters and wider bandwidth, have increased demand for such filters. This filter uses two different Defect Ground Structure (DGS) techniques utilizing the top and ground layers. The first Defect Ground Structure (DGS) technique incorporates two dumbbells and rectangular slots beneath two feed lines, resulting in a unique and modified bandpass filter design. In the second DGS, a series of grooves embedded at three hairpin resonators provide a more compact size and enhanced scattering parameters with wider bandwidth, which is considered an improvement of this design over the existing works. The simulation results use High Frequency Structure Simulator (HFSS) software. Parametric optimization has been conducted; the optimized values of three significant parameters are 4mm length of tap Lt, 0,4mm space between resonators S, and (3×9)mm2 area of rectangular slot (DGS2). The presented filter resonates at 2.5 GHz center frequency with a -3dB fractional bandwidth of 22.4%. The acquired values of insertion loss (S21) and return loss (S11) at the passband are -1.6dB and -54.19dB, respectively, with a flat group delay. The design validity has been verified using Computer Simulation Technology (CST) simulation software and a fabricated prototype. The fabrication results match the simulations excellently, making the suggested filter suitable for various fifth-generation (5G) applications.*

Keywords: *DGS, insertion loss, CST and HFSS, group delay, Vector Network Analyzer (VNA)*

Received: September 8, 2024; Received in revised form: October 20, 2024; Accepted: November 25, 2024

1. INTRODUCTION

In recent days, the applications of wireless communication devices have witnessed increasing requests, which has led to further growth in the microwave device field. Radio Frequency (RF) and microwave filters are excessively utilized in radar systems, satellite communication, recent warfare devices, TV broadcasts, radio broadcasts, and mobile devices. Each wireless communication device operates at various frequencies and allocates various bands for each device [1-6]. Each receiver uses a filter, an essential component that functions as an electronic circuit, allowing a specific range of frequencies to pass while rejecting or attenuating unwanted frequencies. Moreover, filters can be classified according to their characteristics into four different types: lowpass filter (LPF), highpass filter (HPF), bandpass filter (BPF), and bandstop filter (BSF) [7-9]. Therefore, numerous methods exist for designing filters, each with pros and cons. These methods include parallel coupled lines, edge coupled lines, inter-digital lines, comb lines, hairpins, and more.

The hairpin method has the advantage of being small compared to others; it is widely used in filter design [10]. The planar hairpin filter meets the requirements of a compact, high-quality, and low-cost RF/microwave filter. A hairpin BPF passes frequency within a specific extent and rejects or attenuates frequency outside that extent [11]. Also, in hairpin BPF, the hairpin lines comprise folded parallel coupled half-wavelength resonators, which makes the area where parallel lines take up smaller. One of the most common ways to improve filter parameters like insertion loss, return loss, and harmonic suppression is to use a defect ground structure (DGS) [12, 13]. Accordingly, the microstrip technique is used in the hairpin BPF design instead of lumped elements due to its advantages, such as its small size, lightweight, affordability, ease of manufacture, and low loss [14, 15]. Consequently, microwave and RF cir-

cuits use a microstrip line as a means of power transmission. The microstrip line consists of three layers: the top and bottom layers, known as conductor strips and ground, are made from conducting material such as copper, while the middle layer is known as the dielectric substrate [16-20]. Numerous prior researchers have employed the DGS technique to design a hairpin bandpass filter, as seen in [21], where they designed a microstrip hairpin line BPF with two square-shaped DGS. Although this filter has a compact size and good insertion loss (S21), it suffers from low S11 values in the passband region and narrow bandwidth. In [22], a simple filter design for S-band radar incorporates the DGS as a square groove to minimize filter size and suppress harmonics; however, it still struggles with a large occupied area and low return loss (S11). In [23], a planar third-order hairpin BPF employs DGS slot resonators to achieve a high S11 value of -40dB. However, it suffers from a high S21 value and large size. An open stub with DGS employed in [24] is utilized to design a filter for X-band weather radar applications with 120 MHz bandwidth; the S21 value at the passband is -1,57dB. Two different shapes of DGS are utilized to design the hairpin bandpass filter presented in [25], which operates at 2.4GHz and has a moderate return loss of -26dB with sharp roll-off and wide bandwidth in the passband region. In [26], an open loop microstrip structure is used as a DGS to design a three-pole hairpin bandpass filter for a VSAT (Very Small Aperture Terminal) system, with an observed return loss S11 of -13 dB with a triple band at 10.2GHz, 12.2GHz, and 14.8GHz. In [27], a new miniature two-layer bandpass filter is designed that operates at 2.5GHz with a fractional bandwidth of 4.75%; the S21 and S11 values are -1.65dB and -45dB, respectively. From our review of previous studies in the filter design, we found that the DGS technique was used in various geometric shapes and was placed, in most studies, on the bottom layer of the substrate material. However, upon reviewing these studies, it was found that the physical size of most filters was large, the scattering parameter values needed to be higher, and a lack of parametric optimization and traditional hairpin structures were used. These gaps can be addressed by reducing the filter size without affecting its performance, improving the filter's response in terms of scattering parameter values and bandwidth, switching the dielectric material to a low-loss material, conducting a parametric study of several parameters that influence the filter's performance, and modifying the shape and position of the DGS.

The research problem involves improving the scattering parameter values (S11 and S21), obtaining a wider bandwidth in the passband region while maintaining a small size and low cost for the latest compact devices. Filter designers encounter challenges when reducing size, including increased losses, narrower bandwidth, fabrication tolerance sensitivity, and cost. A tradeoff between size reduction with low cost and high performance should be reached. Therefore, in this research, I will study the design of a small-sized filter with unique hairpin-shaped resonators, improving the scattering parameter values, including a parametric optimization of three important parameters that significantly affect the filter's performance (tap length, space between resonators, and rectangular slot area DGS2). This study improves a novel DGS added at the substrate's top and bottom layers, which differs from previous studies and results in enhanced filter performance regarding in-band and out-of-band response, better-scattering parameters, and smaller overall size. The suggested filter has been fabricated and tested to verify the results, and the measured results agree well with the simulated ones. FR4-epoxy is the substrate used, with 4.4 permittivity, 0.02 loss tangent, and 1.6 mm thickness. Sections 2 and 3 arrange the remaining parts. Section 2 provides a brief overview of the design steps of the proposed filter, while Section 3 conducts a parametric study. Then, the simulation results and discussion are presented in Section 4. Section 5 includes the experimental results, followed by Section 6, which compares the proposed filter with other references.

2. PROPOSED FILTER DESIGN

This section will demonstrate constructing a bandpass filter using a three-hairpin resonator with the DGS technique at the top and bottom layers. Fig. 1 displays the equivalent circuit schematic for three resonators at the top layer, which consists of three inductors and capacitors; C12 and C23 represent coupling capacitors between adjacent resonators.

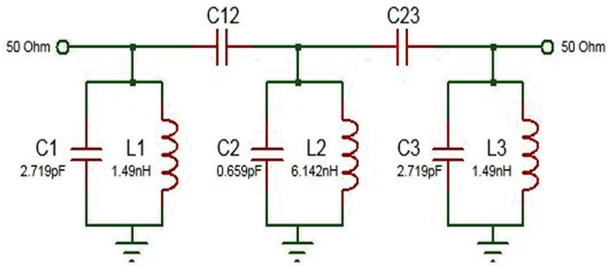

Fig. 1. Lumped elements of the hairpin resonators

The design of a three-pole hairpin bandpass filter aims to strike a balance between performance, size, and selectivity. The shape of the hairpin was chosen mainly for its compactness, easy coupling, and good frequency response. Three hairpin resonators are often chosen instead of five to balance size, complexity, cost, and performance. It is an appropriate choice when moderate bandwidth and selectivity are satisfactory and reducing loss, cost, and size is crucial. A hairpin resonator comprises a U-shaped structure, a substrate, a ground plane, and coupling sections. These parts work together to provide excellent filter performance regarding selectivity, size, and bandwidth. It must first determine the filter and substrate specifications, as shown in Table 1. The FR4 substrate is chosen because it is widely available and cost-effective. The Chebyshev

table will yield the following low pass prototype values for the proposed filter (order three, ripple 0.1, and Chebyshev filter response): $g0 = g4 = 1$, $g1 = g3 = 1.03$, and $g2 = 1.14$. The equations (1-10) were used to design the proposed bandpass filter [8]. The following steps must be followed:

- Step (1), calculate the external quality factor at input and output ports denoted, respectively, by using the following equations (1-2)

$$Q_{e1} = \frac{g_0 g_1}{FBW} \ , Q_{en} = \frac{g_n g_{n+1}}{FBW} \tag{1}$$

$$FBW = \frac{f_h - f_l}{f_o} \tag{2}$$

Where f_h, f_l represents the higher and lower cutoff frequencies, f_o is the center frequency, and FBW is the fractional bandwidth of the filter.

- Step (2), the width of each resonator is calculated by the following equation (3) and (4)

$$B = \frac{60\,\pi^2}{z_c \sqrt{\epsilon r}} \tag{3}$$

$$w/h = \frac{2}{\pi}\left\{\left((B-1)\right) - \ln(2B-1) + \right. \\ \left. + \frac{\epsilon r - 1}{2\epsilon r}\left[\ln(B-1) + 0.39 - \frac{0.61}{\epsilon r}\right]\right\} \tag{4}$$

Where h is the thickness of the FR4 substrate 1.6mm and z_c represents a characteristic impedance equal to 50 ohm, the calculated width of each resonator is 2mm. Furthermore, the resonator length is equal to 16.5mm which is calculated by equations (5-7)

$$k_0 = \frac{2\pi f_0}{c} \tag{5}$$

$$\epsilon_e = \frac{\epsilon r + 1}{2} + \frac{\epsilon r - 1}{2}\sqrt{\frac{1}{1 + 12(h/w)}} \tag{6}$$

$$L = \frac{\frac{\pi}{180^0}}{\sqrt{\epsilon_e} k_0} \tag{7}$$

Where c represents the speed of light in free space 3×10^8 m/s and ϵe is an effective dielectric constant.

- Step (3), calculate the mutual coupling between resonators using equation (8)

$$M_{i,i+1} = \frac{FBW}{\sqrt{g_i g_{i+1}}} \tag{8}$$

The calculated values of two mutual couplings are $M_{12} = M_{23} = 2.067$, the spacing between two adjacent resonators is assumed to be an initial value, and then the filter is designed by using the software simulator HFSS to observe the insertion loss S21 curve and take the two peaks of that curve to calculate coupling coefficients k using equation (9)

$$k = \frac{{f_h}^2 - {f_l}^2}{{f_h}^2 + {f_l}^2} \tag{9}$$

These two peaks on the S21 curve are represented by f_h and f_l, when the value of k is close to the value of M, then the assumed separation distance between adjacent resonators will be considered, equal to 0.4mm in our proposed design.

- Step (4), calculate the tapping point t that represents the position of the feed line at both ports, using equation(10)

$$t = \frac{2l}{\pi}\sin^{-1}\left(\sqrt{\frac{\pi}{2}\left(\frac{z_0}{Q_e z_r}\right)}\right) \tag{10}$$

Where z_0 represents the impedance needed for terminals, z_r impedance for hairpin line, and external quality factor Q_e, the calculated tapping point value is 6mm. Fig. 2 depicts the top layer of the suggested filter, while Table 2 displays its dimensions.

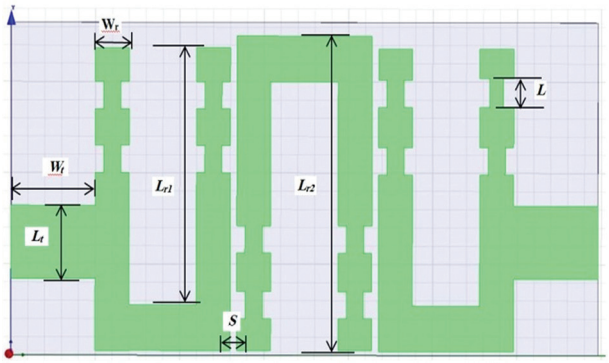

Fig. 2. The top layer of the proposed filter

The -3dB fractional bandwidth measures the filter bandwidth relative to its center frequency (2.5GHz). Where filter bandwidth is 560MHz at -3dB points at the insertion loss (S21) curve. The dielectric constant, thickness, loss tangent, and thermal stability of the FR4 substrate all play a big part in the design of the hairpin resonator. These properties affect how well the filter works. A high dielectric constant leads to more size compactness but reduces the quality factor.

The first DGS is added at the top layer as consecutive grooves with dimensions (0.5×1.5) mm^2 to enhance filter response regarding selectivity with size reduction. On the other hand, the second DGS is employed at the bottom layer of the suggested filter to improve the scattering parameters, which consist of two geometric shapes, as shown in Fig. 3.

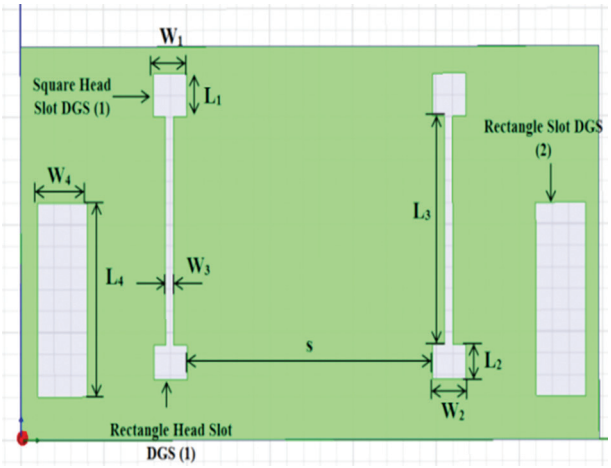

Fig. 3. The bottom layer of the proposed filter

The first one (DGS1) consists of two dumbbells separated by a distance of 14.8 mm. In contrast, the second one (DGS2) consists of a pair of rectangular slots located below the feed lines with dimensions (3×9) mm2, as shown in Fig. 4. These two different DGS techniques differ in their application to the filter design by etching one DGS in the top layer while the other is etched at the bottom layer. Both of them have a simple structure that can be easily implemented. Their impact on the filter includes enhanced scattering parameters, sharper roll-off, and improved passband performance without an increase in the filter size. Table 3 also illustrates all the dimensions of the bottom layer. Fig. 4 displays the ultimate 3D view of the suggested filter.

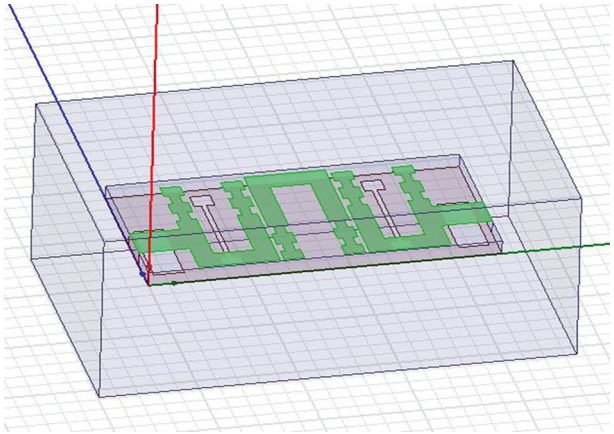

Fig. 4. 3D view of the proposed filter

Table 1. Filter and substrate specifications

Filter parameter	Value
Lower cutoff frequency f_l	2.2GHz
Upper cutoff frequency f_h	2.8GHz
Center frequency f_0	2.5GHz
Order	3
Filter response	Chebyshev
Return loss S11	≤-10
Insertion loss S21	>-2
Substrate type	$FR4_{epoxy}$
Substrate thickness h	1.6mm
Permitivity	4.4
Loss tangent	0.02

Table 2. Top layer dimensions

Filter dimensions (top layer)	Value (mm)
Substrate length	18.25
Substrate width	34.8
Resonator 1 length $Lr1$	16.59
Resonator 2 length $Lr2$	17.25
Resonator 3 length $Lr3$	16.59
Resonator width Wr	2
Tap line length	4
Tap line width	5
Space among three resonators S	0.4

Table 3. Bottom layer dimensions

Filter dimensions (bottom layer)	Value (mm)
Length of square head slot $L1$	2
Width of square head slot $W1$	2
Length of rectangle head slot $L2$	1.6
Width of rectangle head slot $W2$	2
Length of path $L3$	10.6
Width of path $W3$	0.5
Length of rectangle shape slot $L4$	9
Width of rectangle shape slot $W4$	3
Space between two rectangular shape heads (s)	14.8

3. PARAMETRIC STUDY

The suggested filter has been simulated using the finite element method based on HFSS software. This software will provide accurate simulation results, parametric optimization, extraction of the scattering parameters (S11 and S21), and quality factor calculation. The values of insertion loss (S21) and return loss (S11) affect how well the filter works. When insertion loss (S21) is close to zero in the passband region, the signal is attenuated as little as possible. Low return loss (S11 ≤ -10) indicates good impedance matching, and the reflected signal is reduced, which increases the filter's efficiency. The designed filter will experience a series of variations in the tap length, spacing between resonators, and various areas of DGS2. The optimum goal is to get the scattering parameter values (S11 and S21) in an adequate range. The tap length is altered, as shown in Fig. 5, which depicts that the minor increase in tap length changes S11 and S21 values and fractional bandwidth. As shown in the figure, when the tap length increases, the scattering parameter values are enhanced due to sufficient coupling and excellent impedance matching between the resonator and external circuitry. The best return loss (S11) is obtained when Lt is 4 mm, equal to -54.19 dB, as illustrated in Table 4. Optimizing the space between resonators enhances the filter response. The calculated space value S of 0.2mm concerning coupling coefficient k is altered, as indicated in Fig. 6. The figure depicts that the center frequency will not be affected. In contrast, the scattering parameters and fractional bandwidth are noticeably affected, as illustrated in Table 5. The interpretation of this behaviour is that when the resonators are placed close, the coupling increases, increasing the fractional bandwidth and reducing losses due to strong signal transfers between resonators. Finally, the area of the second shape of DGS denoted as DGS2, can be included in the parametric study. The area of that slot is changed from (2×8) mm^2 to (4×10) mm^2 to enhance filter response, as indicated in Fig. 7. The figure indicates a slight effect on the insertion loss (S21), fractional bandwidth, and center frequency. However, Table 6 illustrates a significant impact on the return loss value (S11) when the rectangular slot area equals (3×9) mm2 due to increasing the capacitive and inductive effects when increasing the area of DGS2 and reducing the center frequency.

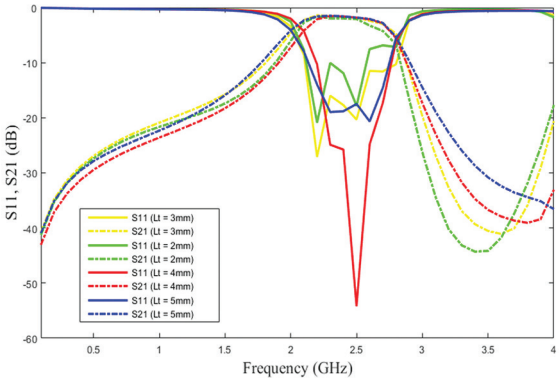

Fig. 5. Simulated S-parameter response when changing the tap length

Table 4. Different tap lengths L_t for the suggested filter

Length of tap Lt (mm)	S21 (dB)	S11 (dB)	Center frequency (GHz)	FBW
2	-1.4, -2	-21, -18	2.2, 2.5	6.8%, 12%
3	-1.4, -1.7	-27, -20	2.35	27%
4 (proposed)	-1.6	-54.19	2.5	22%
5	-1.6	-19, -21	2.5	22.8%

Table 5. The proposed filter comparison based on the spacing between resonators

Space between resonators (mm)	S21 (dB)	S11 (dB)	Center frequency (GHz)	FBW
0.2	-1.4, -3	-30, -23, -15	2.23, 2.8	26%, 4.2%
0.4 (proposed)	-1.6	-54.19	2.5	22.4%
0.6	-1.8	-20, -21	2.5	19.6%
0.8	-2	-23.5	2.5	14%

Table 6. The proposed filter comparison based on the variation of rectangular slot area

Area of rectangular slot (DGS2) (mm)2	S21 (dB)	S11 (dB)	Center frequency (GHz)	FBW
2×8	-1.6	-19, -16	2.5	25.2%
3×9 (proposed)	-1.6	-54.19	2.5	22.4%
4×10	-1.7	-17, -22	2.38	27.3%

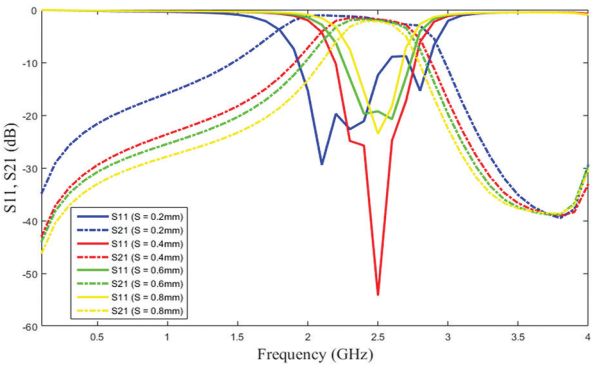

Fig. 6. Simulated S-parameter response when changing space between the resonator

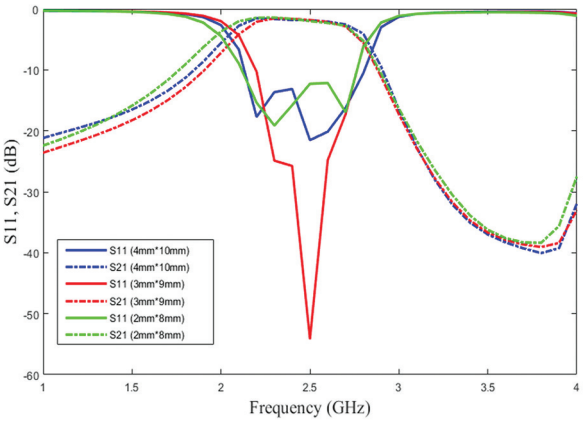

Fig. 7. Simulated S-parameter response when changing the rectangular slot area (DGS2)

4. SIMULATION RESULTS AND DISCUSSION

The proposed filter was initially designed by HFSS software; The results of the simulation for different aspects of the filter design have been extracted, as detailed below:

4.1. VARIOUS MODEL CONSTRUCTIONS

Three models have been designed to demonstrate the effect of DGS on the performance of the filter response. Model 1 incorporates both proposed DGS shapes at both layers. Model 2 encompasses a full ground plane with only defects at the top layer, whereas Model 3 includes top-layer defects and only the first shape of DGS (DGS1) at the bottom layer. Table 7 presents a comparison of the three proposed models. The simulation results for these three models are depicted in Fig. 8. It is clear that the first model has the best scattering parameters (S21, S11) and fractional bandwidth compared to the others, which are -1.6 dB, -54.19 dB, and 22.4%, respectively. Where the lower S11 values are below -10dB, and the closer the S21 values are to zero, the better, as this improves the filter's efficiency. The resonator performance is significantly enhanced by using the second DGS, which leads to improved impedance matching observed when return loss S11 becomes less than -50dB. Furthermore, the second and third models have moderate values for S21 and S11. The center frequency for all three proposed models does not change significantly because the three hairpin resonators at the top layer of the suggested filter have not changed; the only change occurs at the ground layer of the suggested filter.

4.2. CST SIMULATION RESULTS

The CST simulator verifies the results previously obtained from the HFSS. Fig. 9 compares scattering parameters between two software simulators, providing a means to assess the accuracy of the simulated results. The CST simulated results indicate excellent agreement, especially near lower and higher cut-off frequencies, where the lower cut-off frequency is 2.15 GHz and the higher cut-off frequency is 2.7 GHz, with a center

frequency of 2.47 GHz. These variations between the two software are due to several factors, such as the numerical method, boundary conditions and excitations, meshing, and solver technique es.

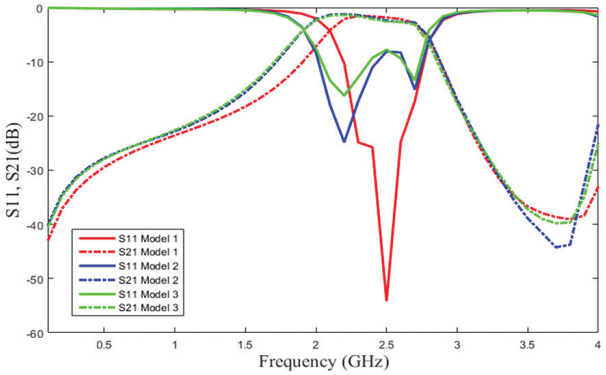

Fig. 8. Simulated S11 and S21 responses of Three different models to demonstrate the effect of DGS

4.3. CURRENT DISTRIBUTION AND GROUP DELAY

The surface current distribution of the proposed filter at the center frequency of 2.5 GHz is indicated in Fig. 10. The filter's surface demonstrates a current flow that appears at the three hairpin resonators in the bandpass region. Another important parameter for the filter design is a group delay, ensuring the signal passes through the filter without distortion and preserving its integrity. This design manages a group delay by optimizing DGS and conducting simulation. The more stable group delay at the passband region, the better. A flat group delay is shown in Fig. 11, which indicates a minimal signal distortion at the passband range.

Table 7. Comparison among three proposed models of the filter design

Model	S21 (dB)	S11 (dB)	Center frequency (GHz)	FBW
model 1 (proposed)	-1.6	-54.19	2.5	22.4%
model 2	-1.3, -3	-25, -15	2.25, 2.7	22.2%, 5.5%
model 3	-1.4, -3	-16, -12	2.25, 2.7	22.2%, 7.4%

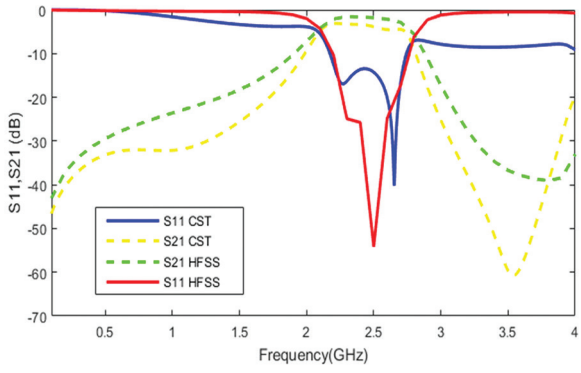

Fig. 9. Simulated S11 and S21 responses of the CST and HFSS simulators for the proposed filter

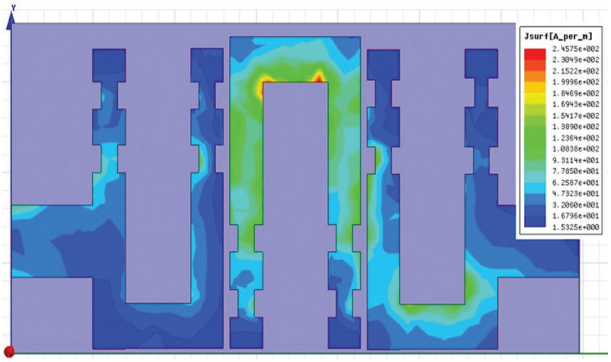

Fig. 10. Surface current distribution of the proposed filter at 2.5GHz

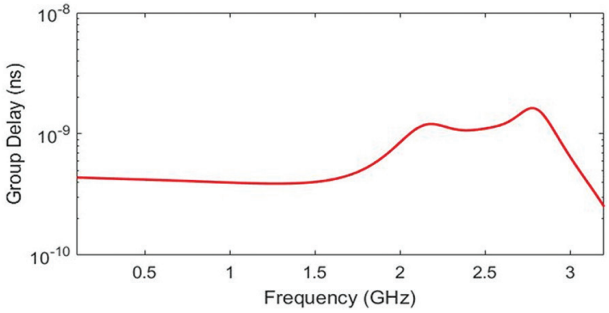

Fig. 11. Group Delay of the proposed filter

5. EXPERIMENTAL RESULTS

The proposed hairpin bandpass filter has been fabricated and tested to verify previously obtained simulation results from CST and HFSS software simulators. The main purpose of verifying the design with CST and the fabricated prototype is to ensure that the theoretical performance of the filter aligns with real-world behaviours. This dual verification process is essential for identifying any discrepancies, design optimization, and impacts of the manufacturing process and ensuring that the final product meets design specifications and industry standards. Fig. 12 illustrates a photograph of the fabricated prototype. Two SMA connectors were utilized to measure the fabricated results. The Vector Network Analyzer (VNA) MS4642A has been used to obtain the measurements, as shown in Fig. 13. A comparison of the simulated and measured results is depicted in Fig. 14. From the figure, it is obvious that there is an outstanding agreement between the simulation and measurement results. Still, slight variations occur due to fabrication tolerance, SMA connector mismatch, substrate material properties, and environmental conditions. Temperature and electromagnetic interference are the two main environmental factors influencing the measurement results. The simulation results achieved a bandwidth of (2.2-2.8) GHz with a center frequency. In measurement results, the bandwidth of (2.4-2.7) GHz with a center frequency of 2.6GHz . The simulated and measured return losses (S11) are -54dB and -30dB for the bandpass region, respectively, while the simu-

lated and measured insertion losses (S21) are -1,17dB and -1,20dB. The challenges encountered during the fabrication process of this filter are pattern precision and variability of substrate material; these were addressed by using engravings with dimensions that are compatible with the cutting machine and simple geometric structures of DGS to avoid design complexity. The proposed filter is appropriate for many modern wireless communication systems that require filters with high selectivity and sharp cut-offs to separate the intended signal band from noise and interference. 5G applications such as enhanced mobile broadband, Internet of Things (IoT), and autonomous vehicles can utilize the suggested filter.

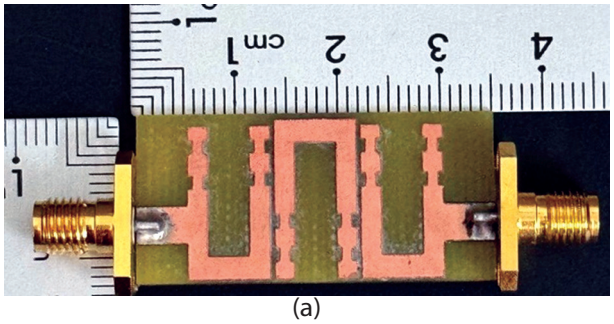

(a)

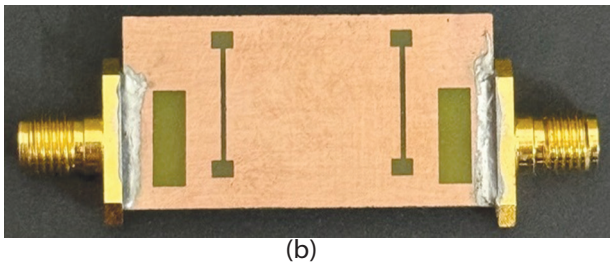

(b)

Fig. 12. Photograph of the fabricated filter. (**a**) Top view, (**b**) Bottom view

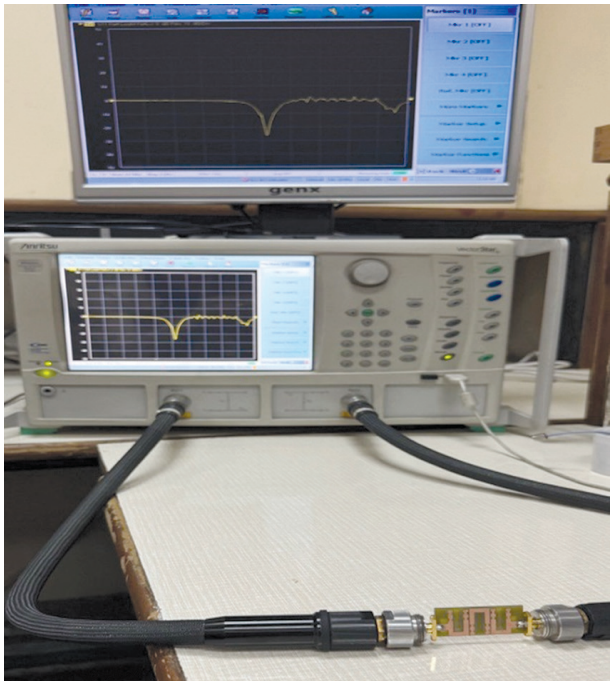

Fig. 13. VNA for measuring the fabricated filter

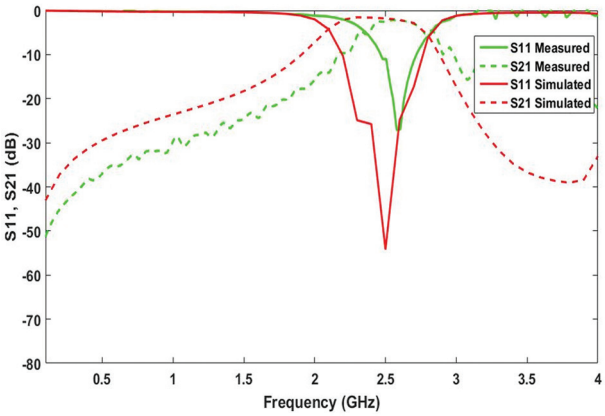

Fig. 14. Comparison between simulated and measured results

6. COMPARISON WITH OTHER REFERENCES

The proposed filter is compared with the other references [21-27] at various ranges of frequency, focusing on insertion loss (S21), return loss (S11), bandwidth, and center frequency highlighted in Table 8. As illustrated in the table, although the suggested filter has a simple structure, it provides the optimum S21, S11, and wider fractional bandwidth equal to -1.6 dB, -54.19 dB, and 22.4%, respectively.

Table 8. Comparison between the proposed filter and other references

Ref No.	Year of pub.	S21 (dB)	S11 (dB)	Bandwidth (BW) (MHz)	Center frequency (GHz)	Filter size $(mm)^2$
[9]	2017	-2.1	-35	389	2.45	40×38
[17]	2018	-1.7	-34	620	2.7	280×140
[19]	2018	-0.37	-34.03	107.4	2.45	20.2×13.3
[21]	2017	-0.2946	-46.64	460	2.22	18.2×34.8
[22]	2018	-0.76	-29	200	3	53.7×17.6
[23]	2019	-3	-41	250	2.35	70×45
[24]	2018	-1.57	-29.9	100	9.5	
[25]	2018	-0.1	-24	600	2.2	49×25
[26]	2021	-1.9, -0.9, -1.2	-13.25, -12.8, -14.72	400, 700, 300	10.28, 12, 14.62	
[27]	2022	-1	-31	130	2.55	21.8×21.6
This Work	2024	-1.6	-54.19	560	2.5	18.25×34.8

7. CONCLUSION

In this paper, a novel hairpin bandpass filter with defective ground structures is analyzed, simulated, and fabricated. 5G applications such as enhanced mobile broadband, Internet of Things (IoT), and autonomous vehicles can utilize the suggested filter. It can also be utilized in wi-fi networks and radar communications. This study utilizes two distinct defect ground structures at the top and bottom layers to enhance the scattering parameters, widen the bandwidth, and maintain compact size. The suggested filter was first created using HFSS software, and a parametric study was highlighted

on the best filter response by changing the space between resonators, the length of the tap, and the area of the rectangular slot (DGS2). The optimized values of three significant parameters are 4mm length of tap Lt, 0,4mm space between resonators S, and (3×9)mm^2 area of rectangular slot (DGS2). The CST simulation results and the fabricated prototype confirm the previous HFSS results. The fabricated prototype's measurement results differed slightly from the simulated ones due to fabrication tolerance and SMA connector mismatch. This filter provides a wider fractional bandwidth of 22.4% in the passband region, excellent return loss (S11) of -54 dB, and insertion loss (S21) of -1.6dB with a short group delay. Future work can apply various ways to the proposed filter to achieve further enhancements such as more miniaturization, conducting parametric optimization with another parameter, and changing the type of substrate material.

8. REFERENCES

[1] E. G. Ouf, E. A. Abdallah, A. S. Mohra, H. El-Hennawy, "Electronically switchable ultra-wide band/dual-band bandpass filter using defected ground structures", Progress In Electromagnetics Research C, Vol. 91, 2019, pp. 83-96.

[2] M.-M. Ma, Z.-X. Tang, X. Cao, T. Qian, "Tri-band cross-coupling bandpass filter with rectangular defected ground structure array", Journal of Electromagnetic Waves and Applications, Vol. 32, No. 11, 2018, pp. 1409-1415.

[3] J. B. Jadhav, P. J. Deore, "A compact planar ultra-wideband bandpass filter with multiple resonant and defected ground structure", AEU - International Journal of Electronics and Communications, Vol. 81, 2017, pp. 31-36.

[4] A. Djaiz, "A new compact microstrip two-layer bandpass filter using aperture-coupled SIR-hairpin resonators with transmission zeros", IEEE Transactions on Microwave Theory and Techniques, Vol. 54, No. 5, 2006, pp. 1929-1936.

[5] L.-H. Hsieh, K. Chang, "Compact, low insertion-loss, sharp-rejection, and wide-band microstrip bandpass filters", IEEE Transactions on Microwave Theory and Techniques, Vol. 51, No. 4, 2003, pp. 1241-1246.

[6] R. P. Verma, B. Sahu, A. Gupta, "A miniaturized UWB bandpass filter with tunable cut-off frequencies employing rectangular open-loop defected ground structure", International Journal of Microwave and Wireless Technologies, Vol. 15, No. 10, 2023, pp. 1689-1697.

[7] E. Sghir, A. Errkik, J. Zbitou, O. Oulhaj, A. Lakhssassi, M. Latrach, "Miniaturized ultra-wideband coplanarwaveguide lowpass filter with extended stop band", Indonesian Journal of Electrical Engineering and Computer Science, Vol. 19, No. 3, 2020, p. 1415.

[8] D. M. Pozar, "Microwave engineering", John Wiley & Sons, 2011.

[9] S. Mora, Y. Alonso, N. Vargas, J. Vera, J. Avendano, "Design of a bandpass filter using microstrip Hairpin resonators", Proceedings of the Chilean Conference on Electrical, Electronics Engineering, Information and Communication Technologies, Pucon, Chile, 18-20 October 2017, pp. 1-5.

[10] A. Ramdedovic, "Tight-coupled microstrip hairpin bandpass filter", Journal of Engineering Research, Vol. 11, No. 1A, 2023.

[11] A. B. Abdel-Rahman, A. K. Verma, A. Boutejdar, A. S. Omar, "Control of bandstop response of Hi-Lo microstrip low-pass filter using slot in ground plane", IEEE Transactions on Microwave Theory and Techniques, Vol. 52, No. 3, 2004, pp. 1008-1013.

[12] N. Abd Wahab, W. N. W. Muhamad, M. M. A. M. Hamzah, S. S. Sarnin, N. F. Naim, "Design a microstrip hairpin band-pass filter for 5GHZ unlicensed WiMAX", Proceedings of the International Conference on Networking and Information Technology, Manila, Philippines, 11-12 June 2010, pp. 183-186.

[13] A. Boutejdar, A. Elsherbini, A. Balalem, J. Machac, A. Omar, "Design of new DGS hairpin microstrip bandpass filter using coupling matrix method", Progress in Electromagnetic Research Symposium, 2007, pp. 261-265.

[14] S.-W. Ting, K.-W. Tam, R. P. Martins, "Miniaturized microstrip lowpass filter with wide stopband using double equilateral U-shaped defected ground structure", IEEE Microwave and Wireless Components Letters, Vol. 16, No. 5, 2006, pp. 240-242.

[15] S. Sun, L. Zhu, "Wideband microstrip ring resonator bandpass filters under multiple resonances", IEEE Transactions on Microwave Theory and Techniques, Vol. 55, No. 10, 2007, pp. 2176-2182.

[16] K. Srisathit, J. Tangjit, W. Surakampontorn, "Miniaturized microwave bandpass filter based on modified hairpin topology", Proceedings of the IEEE International Conference of Electron Devices and Solid-State Circuits, Hong Kong, China, 15-17 December 2010, pp. 4-7.

[17] K. Kavitha, M. Jayakumar, "Design and performance analysis of hairpin bandpass filter for satellite applications", Procedia Computer Science, Vol. 143, 2018, pp. 886-891.

[18] S. A. Shandal, Y. S. Mezaal, M. A. Kadim, M. F. Mosleh, "New compact wideband microstrip antenna for wireless applications", Advanced Electromagnetics, Vol. 7, No. 4, 2018.

[19] S. M. K. Azam, M. I. Ibrahimy, S. M. A. Motakabber, A. K. M. Z. Hossain, "A compact bandpass filter using microstrip hairpin resonator for WLAN applications", Proceedings of the 7th International Conference on Computer and Communication Engineering, Kuala Lumpur, Malaysia, 19-20 September 2018, pp. 313-316.

[20] M. A. Kadhim, M. F. Mosleh, S. A. Shandal, "Wideband Square Sierpinski Fractal Microstrip Patch Antenna for Various Wireless Applications", IOP Conference Series: Materials Science and Engineering, Vol. 518, No. 4, 2019, p. 42001.

[21] V. S. Kershaw, S. S. Bhadauria, G. S. Tomar, "Design of Microstrip Hairpin-Line Bandpass Filter with Square Shape Defected Ground Structure", Asia-Pacific Journal of Electronic and Electrical Engineering, Vol. 1, No. 1, 2017, pp. 21-30.

[22] N. Ismail, T. S. Gunawan, T. Praludi, E. A. Hamidi, "Design of microstrip hairpin bandpass filter for 2.9 GHz-3.1 GHz s-band radar with defected ground structure", Malaysian Journal of Fundamental and Applied Sciences, Vol. 14, No. 4, 2018, pp. 448-455.

[23] M. Nedelchev, A. Kolev, "Synthesis of Planar Filters Using Defected Ground Structure Miniaturized Hairpin Resonators", Engineering, Technology & Applied Science Research, Vol. 9, No. 1, 2019, pp. 3734-3738.

[24] T. Hariyadi, S. Mulyasari, Mukhidin, "Design and Simulation of Microstrip Hairpin Bandpass Filter with Open Stub and Defected Ground Structure (DGS) at X-Band Frequency", IOP Conference Series: Materials Science and Engineering, Vol. 306, No. 1, 2018.

[25] H. Sajjad, A. Altaf, S. Khan, L. Jan, "A compact hairpin filter with stepped hairpin defected ground structure", Proceedings of the IEEE 21st International Multi-Topic Conference, Karachi, Pakistan, 1-2 November 2018, pp. 1-5.

[26] N. Ambati, G. Immadi, M. V. Narayana, K. R. Bareddy, M. S. Prapurna, J. Yanapu, "Parametric Analysis of the Defected Ground Structure-Based Hairpin Band Pass Filter for VSAT System on Chip Applications", Engineering, Technology & Applied Science Research, Vol. 11, No. 6, 2021, pp. 7892-7896.

[27] N. Chami, D. Saigaa, A. Djaiz, "A New Miniature Micro-Strip Two-Layer Band-Pass Filter Using Aperture-Coupled Hairpin Resonators", Engineering, Technology & Applied Science Research, Vol. 12, No. 4, 2022, pp. 9038-9041.